

Using a tensor model for analyzing some aspects of mode-II loading

S. Seitl^{a,*}, D. Fernández-Zúñiga^b, A. Fernández-Canteli^b

^aInstitute of Physics of Materials, Academy of Sciences of the Czech Republic, v. v. i. Žitkova 22, 616 62 Brno, Czech Republic

^bDept. of Construction and Manufacturing Engineering, E.P.S. de Ingeniería de Gijón, University of Oviedo, Campus de Viesques, 33203 Gijón, Spain

Received 19 November 2010; received in revised form 24 March 2011

Abstract

When analyzing the scatter and discrepancies arising among the fracture toughness resulting for different materials and given mixity ratio K_{IIC}/K_{IC} three factors seems to be influential in contributing to the still unsatisfactory state of affairs in this field: a) the lack of established requirements as regards geometry and minimal in- and out-of-plane dimensions of specimens regulating the test for determining mode-II fracture toughness K_{IIC} or, in the more general case, its equivalent in mixed mode cases, b) the role played by the micro-cracking present in the process zone, acknowledged as a microstructural phenomenon already pointed out by Kalthoff and co-workers, needs to be experimentally investigated, and is not considered in the mainly analytical and numerical focussing pursued here, and c) the insufficient attention paid to the particularity of the stress fields around the crack front before and after the daughter crack is formed. In this work, the last question is addressed with the intention of contributing to the clarification of some points with regard to crack instability under mode-II and mixed-mode loading, in particular, why it is difficult to formulate a sufficiently simple failure model for mechanical components or real structures for which the type of load or the geometry results in stress states from which the potential of mixed mode failure arises.

© 2011 University of West Bohemia. All rights reserved.

Keywords: Arcan-Richard specimen, shear mode, crack tip stress field, two-parameter fracture mechanics, fracture parameters, numerical simulation

1. Introduction

The transition of a mode-I crack to a mixed-mode one with the formation of a daughter crack kinked with respect to the original mother crack implies a modification of the stress intensity tensor encompassing different constraint conditions. This emphasizes the significance of analyzing the influence of the constraint conditions before and after the formation of the daughter crack in order to interpret the instability criterion as initiation (before) and the crack growth rate (after) as propagation.

In this work a tensor approach is proposed to consider the real situation of the stress intensity field at the crack. In a certain respect it can be considered an extension of the model handled in [11], in which the existence of different stress intensity factors before and after the crack kinking is underlined indicates that the consideration of the potential mode-I situation in the prospective propagation direction before kinking does not correspond to the regular mode-I state as would be present in the mother crack subjected to mode-I loading. Although the constraint

*Corresponding author. Tel.: +420 532 290 361, e-mail: seitl@ipm.cz.

state for mode II is not thickness dependent, at least in the “before” state, it denotes different constraint conditions than in the case of regular mode-I in the prospective direction.

When analyzing the scatter and discrepancies arising among the fracture toughness resulting for different materials and given mixity ratio K_{IIC}/K_{IC} three factors seems to be influential and to contribute to the continuing, unsatisfactory state of the situation:

- a) The lack of established requirements as regards geometry and minimal in- and out-of-plane dimensions of specimens regulating the test for determining mode-II fracture toughness K_{IIC} or, in the more general case, its equivalent in mixed mode cases. This fact contrasts with the mode-I case, for which linear elastic or small scale yielding fracture mechanics and a state of plane strain dominating at the crack tip are ensured by the requirements made explicit by the ASTM and ESIS standards.
- b) The role played by the micro-cracking present in the process zone, being acknowledged as a microstructural phenomenon already pointed out by Kalthoff and co-workers [7], needs to be experimentally investigated, and is not considered in the mainly analytical and numerical focussing pursued here. This is the reason why the fracture toughness under mode-II K_{IIC} cannot be directly related to that under mode-I K_{IC} .
- c) The insufficient attention paid to the particularity of the stress fields around the crack front before and after the daughter crack is formed. According to the tensor approach proposed in [10] the orientation of the prospective crack necessarily follows the direction predicted using the maximal tangential stress model if initiation is assumed always to succeed under mode-I loading. Further, the transition between the stress fields before and after the kinked (daughter) crack is formed must be taken into consideration [11]. In fact, the stress field, represented by the stress intensity tensor, around the mother crack front before the crack kinks to the prospective direction differentiates from the regular mode-I stress intensity tensor present at the crack front of the daughter crack. The specific features of crack kinking under mode-II and mixed-mode fatigue loading are also recognized and discussed.

In this work, some aspects of the mode-II and mixed-mode problem are handled, in particular, why it is difficult to formulate a sufficiently simple failure model for mechanical components or real structures for which the type of load or the geometry result in stress states from which the potential of mixed mode failure arises.

2. Stress and strain tensors near the crack front under a general load

In the following, the general expression of the stress field in the proximity of the crack front is derived using a tensor approach and then particularized for the cases of pure mode-I and pure mode-II.

2.1. General definitions

The following tensor magnitudes are defined in the stress field [13] $\sigma_{ij}(z, r, \theta; B)$:

- a) Stress intensity field tensor:

$$\phi_{ij}(r, \theta, z; B) = \sqrt{2\pi r} \sigma_{ij}(r, \theta, z; B). \quad (1)$$

b) Spatial stress intensity tensor:

$$k_{ij}^*(\theta, z; B) = \lim_{r \rightarrow 0} \phi_{ij}(r, \theta, z; B) = \lim_{r \rightarrow 0} \sqrt{2\pi r} \sigma_{ij}(r, \theta, z; B). \quad (2)$$

c) Stress intensity tensor:

$$k_{ij}(z; B) = k_{ij}^*(\theta, z; B)|_{\theta=\theta_{cr}} = \lim_{r \rightarrow 0} \sqrt{2\pi r} \sigma_{ij}(r, \theta, z; B)|_{\theta=\theta_{cr}}. \quad (3)$$

d) Spatial constraint tensor corresponding to the second term of Williams' expansion:

$$t_{ij}^*(\theta, z; B) = \lim_{r \rightarrow 0} \left[\sigma_{ij}(r, \theta, z; B) - \frac{k_{ij}^*}{\sqrt{2\pi r}} \right]. \quad (4)$$

e) Constraint tensor:

$$t_{ij}(z; B) = t_{ij}^*(\theta, z; B)|_{\theta=\theta_{cr}} = \lim_{r \rightarrow 0} \left[\sigma_{ij}(r, \theta, z; B) - \frac{k_{ij}^*}{\sqrt{2\pi r}} \right] |_{\theta=\theta_{cr}}. \quad (5)$$

f) Constraint function:

$$\psi_{ij}(r, z; B) = \phi(r, \theta, z; B)|_{\theta=\theta_{cr}} = \sqrt{2\pi r} \sigma_{ij}(r, \theta, z; B)|_{\theta=\theta_{cr}}. \quad (6)$$

Using expressions (2) and (4), the stress tensor σ_{ij} in the proximity of a straight crack tip in a plane normal to the crack front at the point (r, θ, z) for a given specimen thickness B (see Fig. 1) can be expressed in polar coordinates as a Williams' expansion [13]:

$$\sigma_{ij}(r, \theta, z; B) = \frac{k_{ij}(\theta, z; B)}{\sqrt{2\pi}} r^{-1/2} + t_{ij}^*(\theta, z; B) r^0 + O_{ij}(r^{1/2}, \theta, z; B), \quad (7)$$

where O_{ij} represents the remaining higher terms. A justification for the extension of this formula to the component $\sigma_{zz}(r, \theta, z; B)$ is provided in the next subsection.

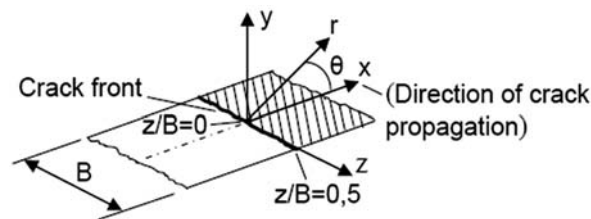


Fig. 1. Crack front and associated coordinate systems (Cartesian and polar)

By identifying (7) with the conventional formulation of Williams' expansion for the general case of mixed-mode I–II, k_{ij}^* can be expressed, indistinctly, in terms of K_I or K_{II} , but considering the preponderance of the mode-II component in the case to be handled, the reference to K_{II} is preferred.

$$\begin{aligned} k_{ij}^*(\theta, z; B) &= K_{II}(z; B) f_{ij}^{(K)}(\theta), \\ t_{ij}^*(\theta, z; B) &= T_{stress}(z; B) f_{ij}^{(T)}(\theta), \end{aligned} \quad (8)$$

where K_{II} is the stress intensity factor for mode-II, defined as $K_{II}(z; B) = \lim_{r \rightarrow 0} \sqrt{2\pi r} \tau_{xy}(z; B)$, T_{stress} is the classical T-stress (see [10, 11]) and $f_{ij}(\theta)$ are the geometric functions with super

index (T) or (K) referred, respectively, to the tensors k_{ij}^* and t_{ij}^* , which can be expressed in terms of the inverse of the mixity ratio $1/\alpha = K_I/K_{II}$ as:

$$\begin{aligned}
 f_{rr}^{(K)} &= \frac{1}{4} \left[\frac{1}{\alpha} \left(5 \cos \frac{\theta}{2} - \cos \frac{3\theta}{2} \right) + \left(-5 \sin \frac{\theta}{2} + 3 \sin \frac{3\theta}{2} \right) \right], \\
 f_{r\theta}^{(K)} &= f_{\theta r}^{(K)} = \frac{1}{4} \left[\frac{1}{\alpha} \left(\sin \frac{\theta}{2} + \sin \frac{3\theta}{2} \right) + \left(\cos \frac{\theta}{2} + 3 \cos \frac{3\theta}{2} \right) \right], \\
 f_{\theta\theta}^{(K)} &= \frac{1}{4} \left[\frac{1}{\alpha} \left(3 \cos \frac{\theta}{2} + \cos \frac{3\theta}{2} \right) + \left(-3 \sin \frac{\theta}{2} - 3 \sin \frac{3\theta}{2} \right) \right], \\
 f_{zz}^{(K)} &= \nu \left(2 \frac{1}{\alpha} \cos \frac{\theta}{2} - \sin \frac{\theta}{2} \right), \\
 f_{rz}^{(K)} &= f_{zr}^{(K)} = f_{\theta z}^{(K)} = f_{z\theta}^{(K)} = 0
 \end{aligned} \tag{9}$$

and

$$\begin{aligned}
 f_{rr}^{(T)} &= \cos^2 \theta, \\
 f_{\theta\theta}^{(T)} &= \sin^2 \theta, \\
 f_{zz}^{(T)} &= \frac{E\varepsilon_{zz}}{T_{stress}} - \nu, \\
 f_{r\theta}^{(T)} &= f_{\theta r}^{(T)} = f_{rz}^{(T)} = f_{zr}^{(T)} = f_{\theta z}^{(T)} = f_{z\theta}^{(T)} = 0,
 \end{aligned} \tag{10}$$

as can be verified from the literature [1, 5, 11, 13]. The extension of these formulae to the component $\sigma_{zz}(r, \theta, z; B)$ is justified in the next subsection.

The critical orientation can be ascertained from the assumption that failure succeeds under mode-I conditions. This condition requires that the stress intensity tensor k_{ij} becomes a diagonal one, what implies that $f_{r\theta} = 0$. The following equation in θ_{cr} is then obtained:

$$\sin \frac{\theta_{cr}}{2} + \sin \frac{3\theta_{cr}}{2} + \alpha \left(\cos \frac{\theta_{cr}}{2} + 3 \cos \frac{3\theta_{cr}}{2} \right) = 0, \tag{11}$$

or

$$\alpha = \frac{\sin \theta_{cr}}{1 + \sin \theta_{cr} - 3 \cos \theta_{cr}} \tag{12}$$

from which after some algebra the value of θ_{cr} can be found in terms of the mixity ratio α resulting from the particular loading case considered. Note that this condition is equivalent to the failure criterion controlled by the maximal tangential stress as proposed by Erdogan and Sih [2].

Accordingly, under pure mode-I loading, i.e., $\alpha = 0$, it results in $\theta_{cr} = 0$ for which

$$k_{ij}(0; B) = K_I(0; B) \begin{vmatrix} 1 & 0 & 0 \\ 0 & 1 & 0 \\ 0 & 0 & 2\nu \end{vmatrix}$$

and

$$t_{ij}(0; B) = T_{stress}(0; B) \begin{vmatrix} 1 & 0 & 0 \\ 0 & 0 & 0 \\ 0 & 0 & \frac{E\varepsilon_{zz}(0;B)}{T_{stress}(0;B)} - \nu \end{vmatrix}, \tag{13}$$

in this case K_I has been referred to by obvious reasons. For pure mode-II, the k_{ij} and t_{ij} tensors can be derived for the mother crack orientation, i.e., $\theta = 0$. In this case, $T_{stress}^{(II)} = 0$ due to the anti-symmetric load and boundary conditions at the crack so that:

$$k_{ij}(0; B) = K_{II}(0; B) \begin{vmatrix} 0 & 0 & 0 \\ 0 & 1 & 0 \\ 0 & 0 & \nu \end{vmatrix} \quad \text{and} \quad t_{ij}(0; B) = \begin{vmatrix} 0 & 0 & 0 \\ 0 & 0 & 0 \\ 0 & 0 & 0 \end{vmatrix}, \quad (14)$$

where K_{II} is now taken as the reference magnitude.

Nevertheless, according to [7] the instability conditions resulting during the failure process, i.e. for $\theta = \theta_{cr} = 70.5$, implies necessarily investigating the stress fields *before* and *after* the secondary or daughter kinked crack is formed. In fact, these two states reveal significantly different stress states.

a) *Before the daughter crack is formed (primarily for crack initiation)*

$$k_{ij}(0; B) = K_{II}(0; B) \begin{vmatrix} 0 & 0 & 0 \\ 0 & 1 & 0 \\ 0 & 0 & \nu \end{vmatrix} \quad \text{and} \quad t_{ij}(0; B) = \begin{vmatrix} 0 & 0 & 0 \\ 0 & 0 & 0 \\ 0 & 0 & 0 \end{vmatrix}, \quad (15)$$

b) *After the daughter crack is formed (primarily for crack propagation)*

$$k_{ij}(0; B) = K_I(0; B) \begin{vmatrix} 1 & 0 & 0 \\ 0 & 1 & 0 \\ 0 & 0 & 2\nu \end{vmatrix}$$

and

$$t_{ij}(0; \theta_{cr}) = T_{stress}(0; B) \begin{vmatrix} \cos^2 \theta_{cr} & 0 & 0 \\ 0 & \sin^2 \theta_{cr} & 0 \\ 0 & 0 & \frac{E\varepsilon_{zz}}{T_{stress}} - \nu \end{vmatrix}. \quad (16)$$

Thus, the tensor approach demonstrates that for pure mode-II loading and consequently for mixed-mode, the stress intensity tensor k_{ij} at the state *before* differs substantially from that corresponding to the state *after*, irrespective of the crack length a , provided the latter is small. This applies not only to the in-plane singularity controlled by k_{rr} and $k_{\theta\theta}$ but also the out-of-plane singularity controlled by k_{zz} . Accordingly, the stress state *before*, i.e., the one supposedly determining the crack instability condition or crack initiation, can be labelled as a *spurious mode-I state*, and cannot be identified with that arising from a regular mode-I failure, as is generally accepted [2]. Further, because the constant stress tensor t_{ij} for pure-mode-II is null, none or negligible in-plane and out-of-plane constraint effects due to specimen thickness or crack ratio are expected, since such an influence could be assigned only to the higher terms of the tensor expansion. This has been confirmed by earlier research performed by Kalthoff and co-workers at the University of Bochum [6, 9] performed on steel and aluminium alloys, see Fig. 2.

In the case of mixed-mode, increasing mode-I participation, i.e., diminishing mixity ratio, promotes the potential influence of the constraint effect, in particular of the specimen thickness on the crack instability.

Once the daughter crack is formed, i.e. for the state *after*, the stress intensity tensor k_{ij} as well as the constant stress tensor recover the structure of the regular mode-I implying the

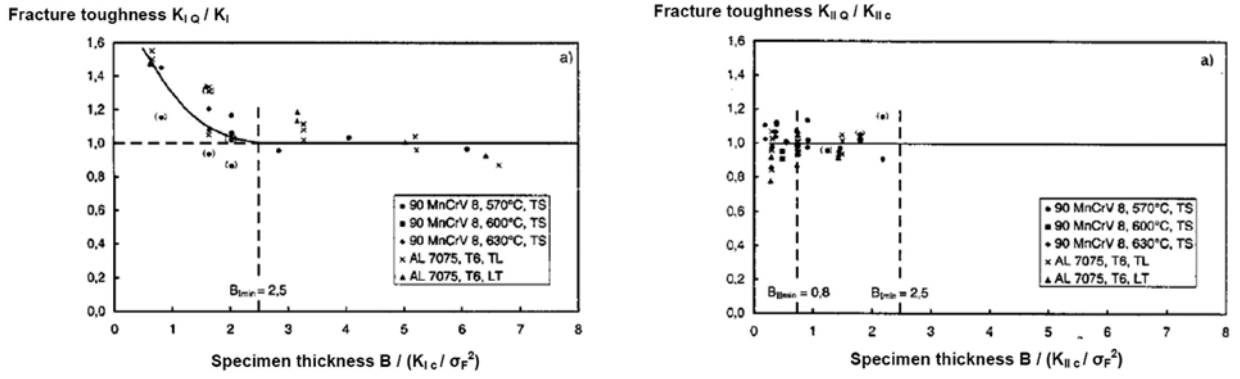


Fig. 2. Dependency and non-dependency of fracture toughness with respect to specimen thickness, respectively, for mode-I and mode-II (from [6])

presence of constraint effects during the crack propagation. In any case, in the first stages of crack propagation the relative size of crack and process zones should have an influence on the crack propagation conditions, an aspect that points out the possible influence of the material fracture properties during the failure sequence. This would explain the different ratios K_{IIC}/K_{IC} observed for different materials, see [12] and [9], and therefore the impossibility of deducing directly K_{IIC} from K_{IC} (see [7]). Since this corresponds to the propagation phase, different crack velocities should be observed for specimens with different thicknesses

2.2. Strain relations at the crack front

So far, the expression of the out-of-plane stress $\sigma_{zz}(r, \theta, z; B)$ has not been justified yet. Applying the generalized Hooke's law $\varepsilon_{ij} = \frac{1+\nu}{E}\sigma_{ij} - \frac{\nu}{E}\sigma_{kk}\delta_{ij}$, allows deriving the expression

$$\varepsilon_{zz}(z, r, \theta; B) = \frac{\sigma_{zz}(r, \theta, z; B) - \nu[\sigma_{rr}(r, \theta, z; B) + \sigma_{\theta\theta}(r, \theta, z; B)]}{E}. \quad (17)$$

According to [4] $\varepsilon_{zz}(z, r, \theta; B)$ cannot be singular in r what implies from (17)

$$\sigma_{zz}(r, \theta, z; B) - \nu[\sigma_{rr}(r, \theta, z; B) + \sigma_{\theta\theta}(r, \theta, z; B)] \neq \infty \quad \text{for } r \rightarrow 0. \quad (18)$$

Accordingly, for any position at the crack front, perhaps with the exception of locations close to $z = \pm B/2$ not considered here, $\sigma_{zz}(r, \theta, z; B)$ must necessarily be singular with the same order of singularity as $\sigma_{rr}(r, \theta, z; B)$ and $\sigma_{\theta\theta}(r, \theta, z; B)$, so that the Williams' expansion is also extensible to

$$\sigma_{zz}(r, \theta, z; B) = \frac{k_{zz}^*(\theta, z; B)}{\sqrt{2\pi r}} + t_{zz}^*(\theta, z; B) + \dots, \quad (19)$$

thus

$$k_{zz}^*(\theta, z; B) = k_{zz}(z; B)f_{zz}^{(K)}(\theta) = K_{II}(z; B)f_{zz}^{(K)}(\theta), \quad (20)$$

validating (7) and (8). From above it follows

$$\varepsilon_{zz}(r, \theta, z; B) = \frac{1}{E} \left[\frac{k_{zz}^*(\theta, z; B) - \nu[k_{rr}^*(\theta, z; B) + k_{\theta\theta}^*(\theta, z; B)]}{\sqrt{2\pi r}} + t_{zz}^*(\theta, z; B) - \nu[t_{rr}^*(\theta, z; B) + t_{\theta\theta}^*(\theta, z; B)] + \dots \right], \quad (21)$$

so that the condition $\varepsilon_{zz}(r, \theta, z; B) \neq \infty$ at the crack front implies

$$k_{zz}^*(\theta, z; B) - \nu[k_{rr}^*(\theta, z; B) + k_{\theta\theta}^*(\theta, z; B)] = 0 \quad (22)$$

and by considering (8) and (9), it follows

$$K_I(z; B)f_{zz}^{(K)}(\theta) - \nu [K_I(z; B)f_{zz}^{(K)}(\theta) + K_I(z; B)f_{zz}^{(K)}(\theta)] = 0 \quad (23)$$

from which finally results (see [10])

$$f_{zz}^{(K)}(\theta) = \nu(f_{zz}^{(K)}(\theta) + f_{zz}^{(K)}(\theta)) = 2\nu \left(\cos \frac{\theta}{2} - \alpha \sin \frac{\theta}{2} \right) \quad (24)$$

and

$$k_{zz}(z; B) = k_{zz}^*(\theta_{cr}, z; B) = K_{II}(z; B)f_{zz}^{(K)}(\theta_{cr}) = 2\nu K_{II}(z; B) \left(\frac{1}{\alpha} \cos \frac{\theta_{cr}}{2} - \sin \frac{\theta_{cr}}{2} \right), \quad (25)$$

as it would be expected from (20).

Since the numerator of the first term of (21) does not depend on r , the following condition must be accomplished:

$$\lim_{r \rightarrow 0} \frac{k_{zz}^*(\theta, z; B) - \nu [k_{rr}^*(\theta, z; B) + k_{\theta\theta}^*(\theta, z; B)]}{\sqrt{2\pi r}} = 0 \quad (26)$$

so disregarding the higher terms in the Williams' expansion that results from (21)

$$\begin{aligned} \varepsilon_{zz}(r, \theta, z; B)|_{r \rightarrow 0} &= \frac{1}{E} [t_{zz}^*(\theta, z; B) - \nu(t_{rr}^*(\theta, z; B) + t_{\theta\theta}^*(\theta, z; B))] = \\ &= \frac{1}{E} \left[t_{zz}(z; B)f_{zz}^{(T)}(\theta) - \nu(T(z; B)f_{rr}^{(T)}(\theta) + T(z; B)f_{\theta\theta}^{(T)}(\theta)) \right] = \\ &= \frac{1}{E} \left[t_{zz}(z; B)f_{zz}^{(T)}(\theta) - \nu T(z; B)(f_{rr}^{(T)}(\theta) + f_{\theta\theta}^{(T)}(\theta)) \right] = \\ &= \frac{1}{E} [t_{zz}(z; B)f_{zz}^{(T)}(\theta) - \nu T(z; B)], \end{aligned} \quad (27)$$

but since $f_{rr}^{(T)}(\theta) + f_{\theta\theta}^{(T)}(\theta) = \cos^2 \theta + \sin^2 \theta = 1$ (see [10]), it results in

$$\varepsilon_{zz}(r, \theta, z; B)|_{r \rightarrow 0} = \varepsilon_{zz}(r, z; B)|_{r \rightarrow 0} = \frac{t_{zz}(z; B) - \nu T(z; B)}{E}, \quad (28)$$

confirming that $\varepsilon_{zz}(\theta)$ is not dependent on θ for $r = 0$.

2.3. Results expected from the analytical

According to the analytical expressions derived for the different orientations of a crack subjected to pure mode-II loading conditions the following results are predicted:

For $\theta = 0$

$$\begin{aligned} k_{xx} &= k_{yy} = 0, \\ k_{xy} &= K_{II}(z; B) = \lim_{r \rightarrow 0} \sqrt{2\pi r} \tau_{xy}(z; B), \\ k_{zz} &= \nu(k_{xx} + k_{yy}) = 0, \\ \varepsilon_{zz}|_{r=0} &= 0, \\ t_{xx} &= t_{yy} = 0, \text{ according to the load and boundary conditions,} \\ t_{zz} &= 0, \text{ according to } \varepsilon_{zz}|_{r=0} = 0 = \frac{t_{zz} - \nu t_{xx}}{E}. \end{aligned} \quad (29)$$

For $\theta = \theta_{cr} = 70.5$ (prospective crack propagation direction)

a) before the daughter crack is formed

$$\begin{aligned}
 k_{rr} &= 0, \\
 k_{zz} &= \nu(k_{rr} + k_{\theta\theta}) = \nu k_{\theta\theta}, \\
 \varepsilon_{zz}|_{r=0} &= 0, \\
 t_{rr} &= t_{\theta\theta} = 0, \text{ according to the load and boundary conditions,} \\
 t_{zz} &= 0, \text{ according to } \varepsilon_{zz}|_{r=0} = 0 = \frac{t_{zz} - \nu t_{rr}}{E}.
 \end{aligned}
 \tag{30}$$

b) after the daughter crack is formed

$$\begin{aligned}
 k_{rr} &= k_{\theta\theta} = 1.155 K_{II}, \text{ irrespective of the specimen thickness} \\
 k_{zz} &= \nu(k_{rr} + k_{\theta\theta}) = 2 \times 1.155 \nu K_{II}
 \end{aligned}$$

In close proximity to the crack front, varying as a function of the specimen thickness B , this results in

$$t_{\theta\theta} = 0, \text{ according to the load and boundary conditions}$$

$$\varepsilon_{zz}|_{r=0} \neq 0 \tag{31}$$

$$t_{rr} \neq 0, \text{ according to the load and boundary conditions}$$

$$t_{zz} \neq 0, \text{ according to } \varepsilon_{zz}|_{r=0} = \frac{t_{zz} - \nu t_{rr}}{E}.$$

3. Numerical calculations

With the aim of checking the analytical expressions found above, finite element calculations were performed using the ANSYS code version for an Arcan-Richard specimen of different specimen thicknesses and crack ratios. The Arcan-Richard specimen and corresponding experimental setup are shown in Fig. 3.

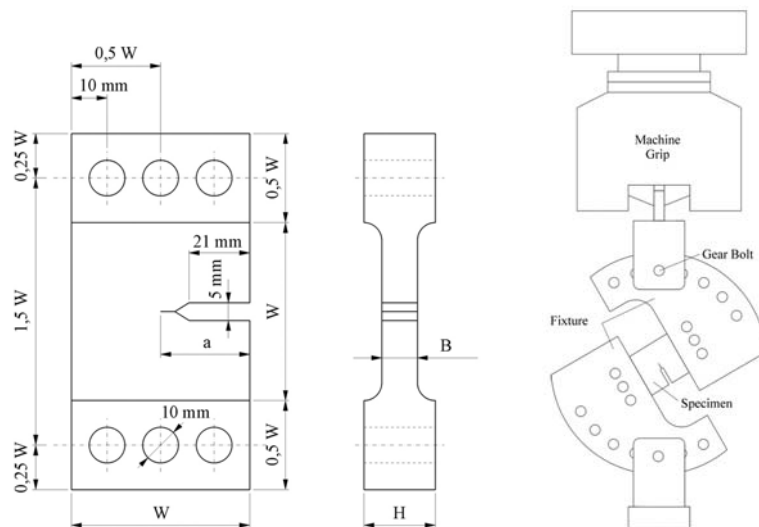


Fig. 3. Arcan-Richard – specimen and Arcan-Richard fixture system, taken from [9]

The specimen dimensions were (see Fig. 3): $W = 50$ mm, $a/W = 0.3, 0.5$ and 0.7 and specimen thickness $B = 5, 10$ and 50 mm. A remote load $P = 100$ N for 2D-plane strain and $P = 100 \times B$ N for 3D model was applied, Young's modulus is $E = 2 \times 10^5$ MPa and Poisson's ratio is $\nu = 0.34$.

4. Results and discussion

The stress intensity factor K and the T-stress values were computed by means of the finite element method and using the stress difference method [14]. As a first step, the 2D finite element method solution was employed on the Arcan-Richard specimens to verify the accuracy of the numerical model used. A typical finite element mesh and the boundary conditions used in the computations are shown in Fig. 4 together with a detailed view of the small region near the crack tip. The size of the smallest element in the crack tip is 5×10^{-5} mm.

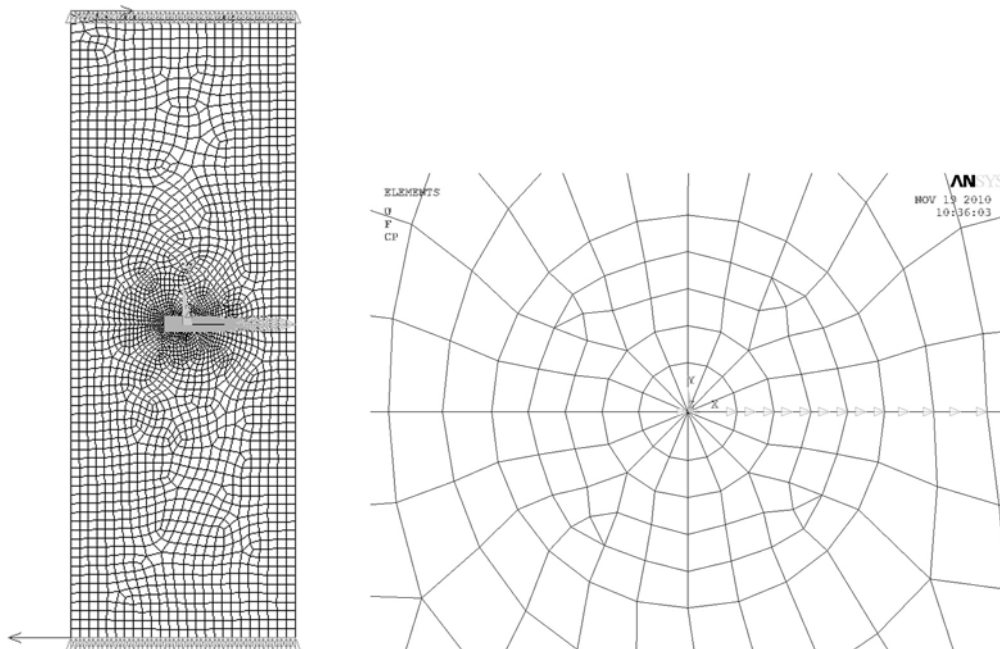


Fig. 4. Load application and finite element mesh used in the finite element calculations: detailed view of the small region near the crack tip

The analytical expressions deduced for the components of the stress intensity tensor k_{ij} and those for the constant tensor t_{ij} should be validated by the numerical calculation, first for the initial crack direction $\theta = 0$ then for the prospective crack propagation direction $\theta = \theta_{cr}$ for both of the states: *before* and *after* the daughter crack is formed. In this work, only a selected number of components have been considered, see section 4. The comparison of data from literature (e.g. [8]) and from our numerical 2D-model (plane strain) is shown in Fig. 5 the data are in good relation; the differences are smaller than 2%. The influence of specimen thickness on the fracture toughness is shown in the Fig. 6.

The real test conditions applied the Arcan-Richard specimen do not correspond an ideal simulation of the mode-II test presented here. The influence of grips will be studied later, see Fig. 3. As a result, the out-of-plane stress intensity component for $\theta = 0$, $k_{zz}^*|_{\theta=0}$, is zero as predicted, $k_{zz}^*|_{\theta=0} = 2\nu K_I = 0.68 K_I$, i.e., $K_I = 0$ MPa m^{1/2}. The same conclusions are for t_{xx} and t_{zz} , as well, see Fig. 7 for t_{xx} stress component. Finally, note that critical crack orientation

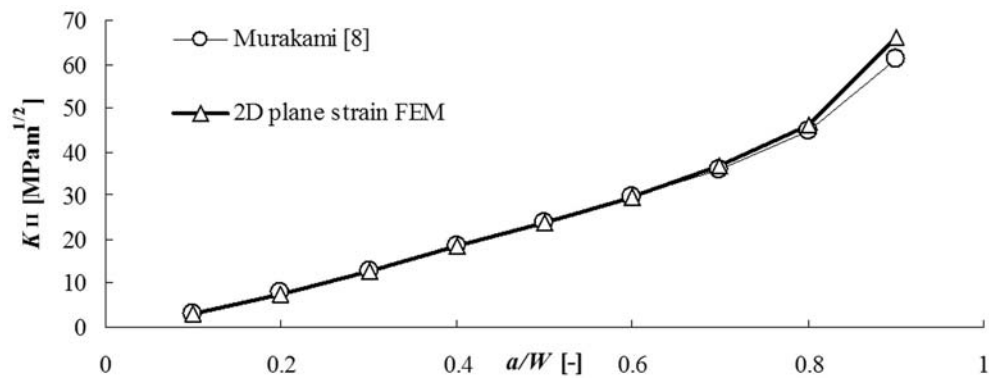


Fig. 5. Comparison of results from the used numerical model with the literature data [8]. The loading force $P = 100$ N

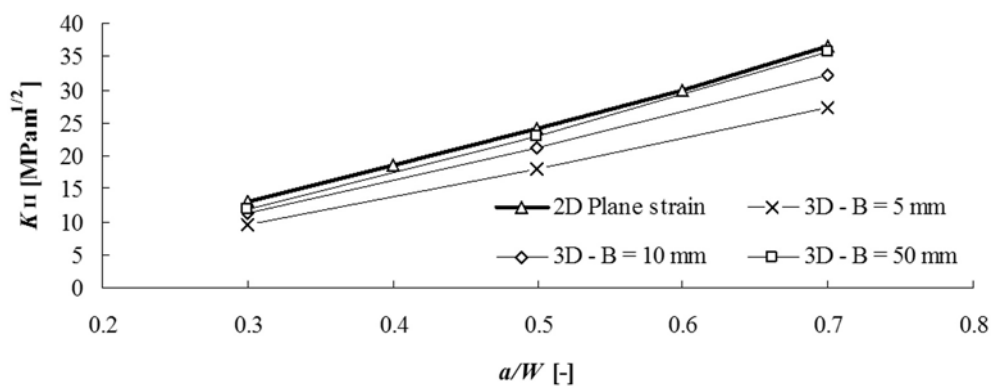


Fig. 6. Results of the stress intensity factors K_{II} for the A-R specimen under expectedly mode-II conditions for different specimen thickness and crack ratios. The loading force $P = 100 \times B$ N

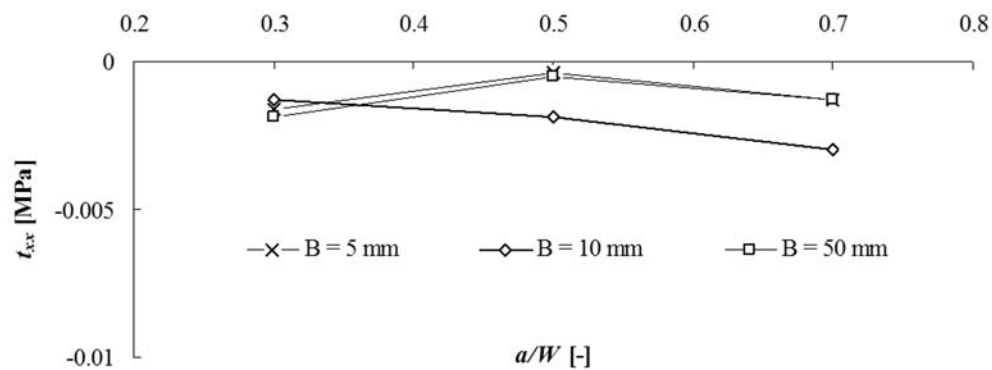


Fig. 7. Example of results of the t_{xx} stress components for the A-R specimen under mode-II conditions for different specimen thickness and crack ratios

from MTS — criteria [4] is $\theta_{cr} = 70.5$ but in reality this can be influenced by an existence of non zero mixity ratio $\alpha = K_{II}/K_I$, equation (12). Consequently, $k_{\theta\theta}^*|_{\theta=70.5}$ will be zero as predicted. A more extensive numerical calculation must be performed if a detailed checking of the analytical results expected according to the sets (29), (30) and (31) are pursued.

The role played by the micro-cracking present in the process zone, being acknowledged as a microstructural phenomenon and already pointed out by Kalthoff and co-workers, needs to be experimentally investigated, and is not considered in the mainly analytical and numerical

focusing pursued here. This might be a reason why the fracture toughness under mode-II K_{IIC} cannot be directly related to that under mode-I K_{IC} . All this evidences the necessity of standardizing the specification of minimum specimen sizes for determining the true valid values of fracture toughness under mode-II and mixed-mode loading as suggested in [3,4].

5. Conclusion

The main conclusions of this work are the following:

- A tensor approach is applied to derive the general analytical expressions of the stress and strain state for mixed-mode conditions I–II at the crack front of Arcan-Richard specimens encompassing as particular cases pure mode-I, pure mode-II conditions.
- For pure mode-II, the approach confirms two different stress and strain fields at the crack front before and after the daughter crack forms implying also different in-plane and out-of-plane constraint conditions in the crack surrounding. This also applied to mixed-mode conditions.
- For the earlier state, a spurious mode-I state prevails in the prospective crack propagation direction θ_{cr} characterized by a zero stress intensity tensor component k_{rr} that one presumably governing the crack initiation conditions. Near the crack front, no influence of the specimen thickness on the constraint conditions is observed, and therefore no influence of specimen thickness on the fracture toughness is expected as long as a pure mode-II stress state prevails along the initial crack direction $\theta = 0$. This is confirmed by earlier external research performed on steel and aluminium alloys.
- As soon as the daughter crack forms, i.e., in the so-called state after, a regular mode-I stress state arises at the crack front. Constraint effects are observed as a result of the specimen thickness and the influence of specimen thickness on the fracture toughness is to be expected.
- As a result of the presence of a mode-I component, the influence of the specimen thickness B and crack ratio a/W , though small, is noticeable both in the results of the component k_{zz} and of the t_{ij} components, t_{rr} and t_{zz} that are close to zero.
- Further calculations are envisaged to analyze the stress relations in the state after, particularly in matters concerning constraint evolution during the crack growth process.
- The analytical derivations and the numerical calculations prove the utility of the tensor approach proposed in this work.

Acknowledgements

The authors acknowledge partial economical support from FYCIT, Project IB08-171 and from the Spanish Ministry of Science and Innovation, Project DPI 2007-66903, Academy of Sciences of the Czech Republic, project M10041090 and Czech Science Foundation, projects 101/09/0867 and P108/10/2049.

References

- [1] Anderson, W. L., *Fracture mechanics, fundamentals and applications*, CRC Press, 3rd. Edition, 2004.
- [2] Erdogan, F., Sih, G. C., On the crack extension in plates under plane loading and transverse shear, *Journal of Basic Engineering*, Transactions of ASME, 1963, pp. 519–527.
- [3] Fernández-Zúñiga, D., Fernández-Canteli, A., Doblaré, M., Kalthoff, J. F., Bergmannshoff, D., Novel test criteria for determining fracture toughness under pure mode-II and mixed-mode loading, XIV European Conference of Fracture, Krakow (Polonia), Vol. I, 2002, pp. 521–530.
- [4] Fernández-Canteli, A., Castillo, E., Fernández-Zúñiga, D., Linear elastic fracture mechanics based criteria for fracture including out-of-plane constraint effect, Submitted to *Theoretical and Applied Fracture Mechanics*.
- [5] Giner, E., Fernández-Zúñiga, D., Fernández-Sáez, J., Fernández-Canteli, A., On the J_{x1} -integral and the out-of-plane constraint in a 3D elastic cracked plate loaded in tension. *Int. J. of Solids and Structures* 47, 2010, pp. 934–946.
- [6] Hiese, W., *Gültigkeitskriterien Zur Bestimmung Von Scherbruchzähigkeiten*, Doctoral Thesis, Ruhr-Universität Bochum, 2000.
- [7] Kalthoff, J. F., Fernández-Canteli, A., Blázquez, A., Fernández-Zúñiga, D., Singular stress fields and instability Conditions for mode II and mixed-mode loaded cracks, *Strength, Fracture and Complexity* 4, 2006, pp. 141–160.
- [8] Murakami, Y. et al. *Stress Intensity factors*, Handbook, Pergamon Press, 1998.
- [9] Podleschny, R., *Untersuchungen zum Instabilitätsverhalten scherbeanspruchten Risse*, Doctoral Thesis, Institut für Mechanik, Ruhr-Universität Bochum, 1995.
- [10] Seitzl, S., Knésl, Z., Two parameter fracture mechanics: fatigue crack behaviour under mixed mode conditions. *Engng. Fract. Mech.* 72, 2008, pp. 857–865.
- [11] Smith, D. J., Ayatollahi, M. R., Pavier, M. J., On the consequences of T-stress in elastic brittle fracture, *Proc. R. Soc.* 462, 2006, pp. 2 415–2 437.
- [12] Tenhaeff, D., *Untersuchungen zum Ausbreitungsverhalten von Rissen bei überlagerter Normal- and Schubbeanspruchung*, Doctoral Thesis, Universität Kaiserslautern, 1987.
- [13] Williams, M. L., On the stress distribution at the base of a stationary crack, *J. Appl. Mech.* 24, 1957, pp. 109–114.
- [14] Yang, B., Ravi-Chandar, K., Evaluation of elastic T-stress by the stress difference method, *Engineering Fracture Mechanics* 64, 1999, pp. 589–605.